

Field Emission from Metals into Alkali Halide Crystals*

M. GELLER†

Laboratory for Insulation Research, Massachusetts Institute of Technology, Cambridge, Massachusetts

(Received December 8, 1955)

The transient photocurrents associated with the movement of photoelectrons in additively colored alkali halide crystals, and the accompanying growth of positive space charge at the cathode leading to field emission, has been previously calculated and verified by room-temperature measurements. These experiments have been extended to low temperatures and the theory has been expanded to include the final photocurrents produced by the space-charge enhanced field.

From measurements of the initial current, its time constant, and of the final current, a field strength at the cathode can be derived and correlated to the final current density. Fowler-Nordheim plots yield a straight line, as expected for field emission,

but the order of magnitude of the calculated field and the "apparent" work function are too small to be reasonable. The work function furthermore exhibits a dependence on light intensity. The field emission should be nearly independent of temperature, and this is verified. The photocurrent decreases from room temperature to -130°C by a factor of only two; this decrease can be attributed to the lowered mobility of the electrons in the crystal. Final photocurrent *vs* voltage curves for various metals and composite surfaces indicate that the photocurrent is controlled by the ionized *F*-centers in a thin surface layer of the crystal and that the image forces of these centers create the high fields required for the emission.

STUDIES of the prebreakdown currents in alkali halide crystals¹ and of the dependence of the breakdown voltage on electrode material and rise-time of applied voltage,² established the importance of electron emission and of field distortion by space charge for the electric breakdown strength. A detailed investigation of space charge buildup and field emission became possible by the use of additively colored alkali halide crystals, in which the frozen-in electrons can be mobilized by light absorption. The theoretical behavior of such a system was studied and a first experimental investigation made at room temperature.³ The purpose of the present paper is to extend this study and to examine the electron emission from the cathode in such a space-charge enhanced electric field in detail as a function of temperature and electrode material.

SPACE-CHARGE LIMITED PHOTOCURRENTS IN COLORED ALKALI HALIDE CRYSTALS

The initial transient phenomenon, the decay of the photocurrent with time when electrons can leave the crystal at the anode but not enter at the cathode, has been calculated previously in detail.³ A final steady-state equilibrium photocurrent results when electrons are released from the cathode, and the number entering per second equals the number leaving per second at the anode.

As in the transient calculation we assume that in the final equilibrium state for a stationary photocurrent, two regions in the crystal can be distinguished (Fig. 1): (a) A neutral, unbleached region II of constant field strength in front of the anode and (b) a region I, con-

taining the positive space charge and extending from the cathode, $x=0$, to a distance d ($d \leq d_{\infty}$). This section, completely bleached without field emission, will be only partially bleached because some *F*-center traps capture electrons from the emission current. The net charge density is

$$\rho(x) = \rho_0 - \rho_e(x), \quad (1)$$

where $\rho_0 = N_0e$ is the positive space charge of ionized *F* centers and $-\rho_e(x)$ the negative space charge stemming from the final current density J_F . According to Stokes's law, $J_F = \rho_e bE$, and hence

$$\rho(x) = \rho_0 - (J_F/bE). \quad (2)$$

Let the potentials be

$$\begin{aligned} V &= 0 & \text{at } x=0, \\ &= V_0 & \text{at } x=l, \\ &= V' & \text{at } x=d, \end{aligned} \quad (3)$$

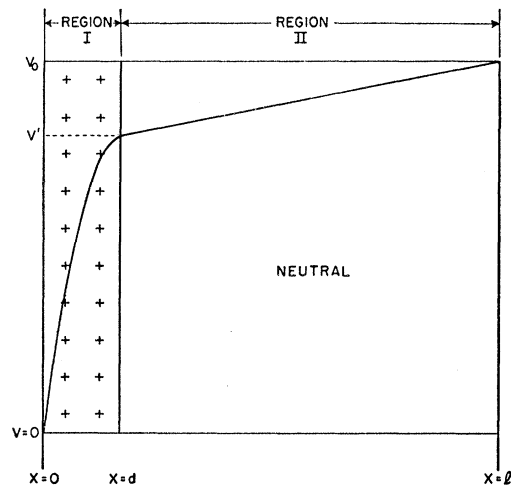


FIG. 1. Voltage distribution in equilibrium state of a stationary photocurrent.

* Sponsored by the Office of Naval Research, the Army Signal Corps, and the Air Force. Reproduction of this article in whole or in part is permitted for any purpose by the United States Government.

† Present address: Hughes Aircraft Company, Semiconductor Laboratory, Los Angeles, California.

¹ A. R. von Hippel, Phys. Rev. **54**, 1096 (1938).

² A. von Hippel and R. S. Alger, Phys. Rev. **76**, 127 (1949).

³ von Hippel, Gross, Jelatis, and Geller, Phys. Rev. **91**, 568 (1953).

and the ratio of final to initial current

$$K \equiv I_F / I(0). \tag{4}$$

At $t=0$, without field distortion, as well as after a final photocurrent is established, the currents are proportional to the field in the neutral region II:

$$\begin{aligned} I_0 &\propto V_0/l, \\ I_F &\propto (V_0 - V')/(l-d), \\ V' &= V_0[1 - K(l-d)/l]. \end{aligned} \tag{5}$$

The field in region II is

$$E_2 = -KV_0/l, \tag{6}$$

that is, K represents the reduction factor for the applied field, V_0/l , in region II, caused by the space charge in region I.

For region I, it follows from Poisson's equation that

$$\partial E / \partial x = (\rho_0 - \rho_e) / \epsilon'. \tag{7}$$

With Eq. (2), this gives

$$\epsilon' E \partial E / \partial x = \rho_0 E - (J_F/b). \tag{8}$$

Experimentally, it is found that the term J_F/b is small compared to the other; hence, if in a first approximation b is independent of x ,

$$\frac{1}{2} \epsilon' E^2 = -\rho_0 V - (J_F x/b) + \text{constant}. \tag{9}$$

With the boundary conditions [see Eq. (3)] at $x=d$, $V=V'$, $E=E_2$, we obtain

$$\frac{1}{2} \epsilon' E^2(x) = \frac{1}{2} \epsilon' E_2^2 + \rho_0 [V' - V(x)] - (J_F/b)(x-d). \tag{10}$$

For the field at the cathode [at $x=0$, $V=0$, $E(x)=E_c$],

$$E_c^2 = E_2^2 + (2\rho_0 V' / \epsilon') - (2J_F d / \epsilon' b). \tag{11}$$

For $t=0$, the field is linear and the initial current density

$$J_0 = -b\rho_0 V_0/l \tag{12}$$

and

$$J_F = -Kb\rho_0 \frac{V_0}{l}. \tag{13}$$

Hence

$$E_c = - \left\{ \left[\frac{KV_0}{l} \right]^2 + \frac{2\rho_0 V_0}{\epsilon'} (1-K) \right\}^{\frac{1}{2}}. \tag{14}$$

Eliminating ρ_0 , the color concentration density, by referring to the initial current density $I(0)/A_0$ and the time constant τ of its decay as³

$$\rho_0 = \frac{2}{V_0 \epsilon'} \left[\frac{I(0)\tau}{A_0} \right]^2, \tag{15}$$

the stationary field at the cathode may be rewritten as

$$E_c = - \left\{ \left[\frac{KV_0}{l} \right]^2 + \left[\frac{2I(0)\tau}{\epsilon' A_0} \right]^2 (1-K) \right\}^{\frac{1}{2}}. \tag{16}$$

APPARATUS AND MEASUREMENT TECHNIQUE

Sample Holder

The sample holder was a vacuum Dewar vessel (Fig. 2), in which the crystal was pressed by a high-voltage spring electrode against a copper block. This block, the low-voltage electrode, was separated from the coolant and the heater by a quartz crystal (0.03 in. thick) cut perpendicularly to the optical axis for electrical insulation and thermal conduction. With liquid nitrogen as the coolant, the crystal could be maintained at any temperature from -170°C (no heater current) to -100°C . The temperature of the crystal was measured by a thermocouple mounted on the copper block and calibrated by couple inserted into a small hole of a sample crystal. The temperature drop across the crystal was at no time greater than 1°C .

To obtain low temperatures in vacuum, the sample and copper block were surrounded by a thermal shield of copper.

Current Amplifier

To measure and record the current as a function of time, a modified version of a Roberts's feedback microammeter,⁴ designed by Mr. D. A. Powers of this laboratory, was used to drive a G.E. photoelectric recorder and a Dumont 304 A oscilloscope. As the time constant of the former is about 0.1 sec, the oscilloscope was needed for photographing the initial rapid decay of the current.

Currents from 10^{-15} to 10^{-5} amp could be measured

⁴ S. Roberts, Rev. Sci. Instr. 10, 181 (1939).

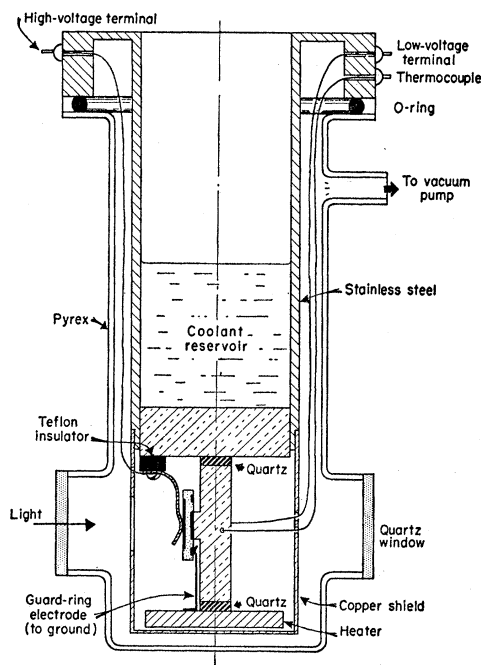


FIG. 2. The vacuum Dewar sample holder.

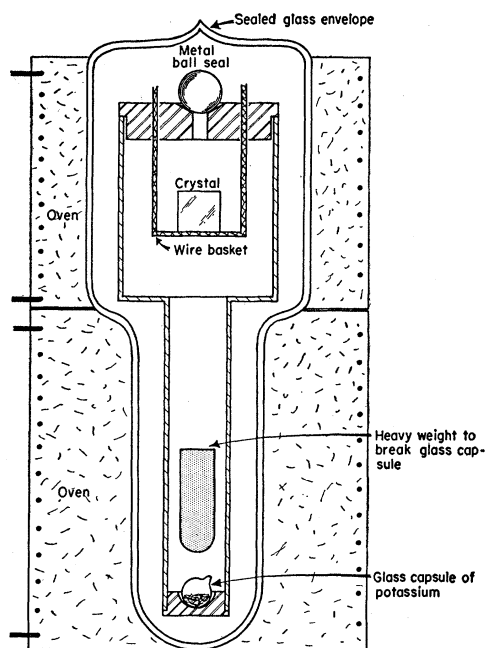


FIG. 3. Crystal coloration equipment.

by changing the value of the input resistance in steps of 10^3 . Below 10^{-13} amp the accuracy was 10%, at higher currents better than 5. The input resistances were calibrated against a standard capacitance in an RC circuit, using a string electrometer as a voltmeter. The zero drift of the amplifier was smaller than 2% of full scale per day.

The measurement of time constants presupposes a minimum of distortion of the photocurrent wave form by the amplifier. For currents smaller than 10^{-10} amp, the response of the amplifier was limited by the charging of the self-capacitance of the input resistance. Fortunately, in this range the voltages applied were small and the photocurrents decayed slowly. At higher current levels the response was limited by an RC filter in the first stage, inserted to eliminate oscillations. Discharging of a standard RC circuit through the input showed that the amplifier was reliable for time constants $\geq 10^{-3}$ sec.

Power Supply

The main power supply consisted of sixteen 300-v (U-200 Burgess) batteries, mounted in a shielded metal container. Voltages of 300, 600, 1200, 2400, 3600, 4800 v of either polarity were thus available. At no time were the currents greater than 10^{-5} amp; the voltages were checked by an electrostatic voltmeter.

Light Source

A 750-watt G.E. air-cooled projection bulb (T12P-120 v) served as the white light source. The current through the lamp, stabilized by a voltage regulator, was kept to one-half of rated value. Even after one year of

operation, no visible blackening of the envelope occurred by tungsten evaporation.

The light intensity was reduced by neutral density filters⁵ constructed of 100-mesh brass wire screens in tandem. The light intensity could be increased by a factor of 8 ($L=8$) by focusing the filament with a spherical mirror (5 in. diam) on the sample. An infrared filter (Chance ON-25), with cutoff at 1.5μ , in front of the entrance window of the sample holder, shielded the copper block against heat radiation.

Crystal Preparation

Single crystals of KBr (one-inch cubes, Harshaw) were additively colored in the apparatus shown in Fig. 3 by potassium, purified by distillation. Before sealing off the Pyrex envelope, the system was evacuated and baked for one day at 500°C . The coloration proceeded in a two-stage oven. The crystal was maintained at a temperature of 570°C and the temperature of the potassium, which determines the concentration of F centers, adjusted between 275° and 325°C .

Thin sections ($\frac{1}{2}$ to 2 mm) were split from the large colored crystals and electrodes immediately deposited on the freshly cleaved faces in a vacuum of 10^{-5} mm. The electrode system with guard ring (Fig. 4) guaranteed that the currents measured were not surface currents. A bare strip on each edge, $\frac{1}{16}$ in. wide, separated the high voltage from ground and increased the leakage path. The effective area of this three-electrode system was 1.35 cm^2 .

RESULTS

The movement of the electron cloud at room temperature as a function of light intensity, applied voltage, crystal length, and color-center concentration has been previously established.³ The equations developed proved to be a good, first approximation. In Secs. 1 to 3, we will add details not given previously, and refer to aspects which are a prerequisite for the understanding of later sections.

1. Mobility Data

The mobility of the electrons can be determined by a measurement of $I(0)^3$ and τ as

$$b = \epsilon' A_0 l / 2I(0)\tau^2. \quad (17)$$

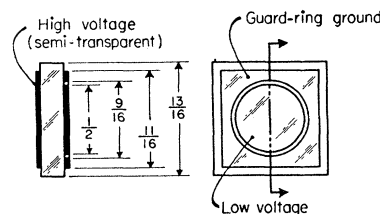


FIG. 4. Crystal electrodes.

⁵ L. J. Heidt and D. E. Bosley, J. Opt. Soc. Am. 43, 760 (1953).

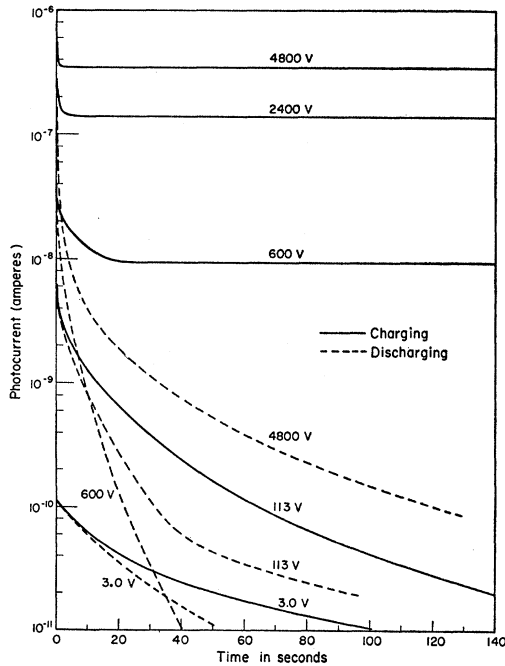


FIG. 5. Charging and discharging characteristics at a constant light intensity.

Its values as a function of light intensity are listed in Table I.

Within the accuracy of the data, the mobility is proportional to the light intensity; it decreases with temperature because we are concerned with a trapping and release process.⁶ The product, quantum efficiency times the Schubweg (ηw), drops sharply,⁷ and it is this factor which predominates.

2. Dark Currents as a Function of Temperature

The dark current was measured before illumination, at room temperature as well as at low temperature. The currents varied linearly with the applied voltage. The conductivity decreased by a factor of 400 as the temperature dropped from room temperature to -130°C .

3. Charging and Discharging Characteristics

Figure 5 shows $\log I$ of charging and discharging currents as a function of time, at a constant light in-

TABLE I. Mobility as a function of light intensity.

Temperature	Light intensity L	b ($\text{m}^2 \text{v}^{-1} \text{sec}^{-1}$)
-170°C	1	$(5 \pm 2) \times 10^{-10}$
	0.1	$(6 \pm 3) \times 10^{-11}$
	0.01	$(9 \pm 5) \times 10^{-12}$
-130°	0.1	$(1.1 \pm 0.6) \times 10^{-10}$
	1	$(1.0 \pm 0.3) \times 10^{-8}$
Room temp.	0.1	$(1.8 \pm 0.3) \times 10^{-9}$

⁶ A. von Hippel, J. Appl. Phys. 8, 815 (1937).

⁷ G. Glaser, Nachr. Ges. Wiss. Göttingen Math.-physik. Kl., Fachgruppe II 3, No. 2, 31 (1937).

tensity, for various voltages. The initial portions of the charging curves are straight lines. This, as the theory shows, represents the motion of the electron cloud. The time constants of these straight-line segments were in the range of 0.01 to 1 sec. The deviation from the straight lines indicates the appearance of electron emission from the cathode. At low voltages, the electron cloud moves slowly, the currents decay gradually and bend around to a steady value. At higher voltages, the currents decay quickly in the larger driving field and bend sharply to a final value.

The discharge currents strikingly exhibit the effect of field emission. When low charging voltages preceded, they follow the charging characteristics rather closely. At higher voltages, the initial currents are different, and the decay of the discharge current is more rapid

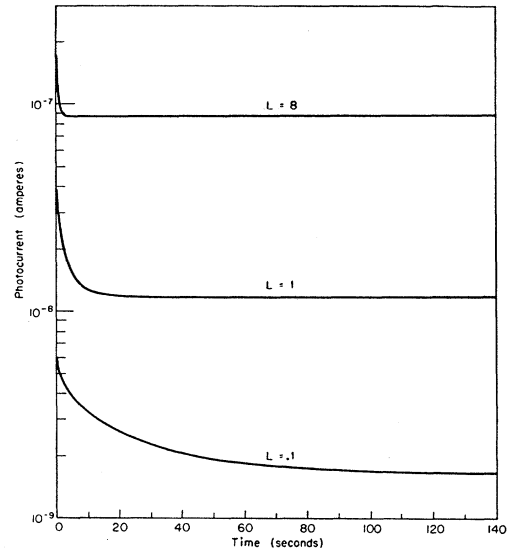


FIG. 6. Charging characteristics at a constant voltage.

than that of the charging current. At the beginning of the discharge, at the cathode there is still the space-charge layer which was responsible for the final current I_F . The current measured at $t=0$, at the beginning of the discharge, is due to the motion of the electron cloud as it retraces its path to reduce the positive layer, plus the emission current I_F flowing in the opposite direction: $I(0)_{\text{discharging}} = I(0)_{\text{charging}} - I_F$. This is a particular case of the law of superposition,⁸ as verified by the data of Table II.

The final equilibrium state after discharge is a neutral central section with a bleached region of height $\frac{1}{4}V_0$ in front of both electrodes.³ For large values of the applied voltage, the space-charge fields formed may be sufficiently large to draw electrons into the crystal. If there is any asymmetry in the emission properties of the two metal electrodes, current reversals of a small magnitude

⁸ A. R. von Hippel, Dielectrics and Waves (John Wiley and Sons, Inc., New York, 1954), p. 232.

may occur. This is observed, for example, in the discharge curve for 600 volts (Fig. 5). The two electrodes here were gold and aluminum.

Figure 6 illustrates charging characteristics at a constant voltage (600 v) for different light intensities. The decay of the currents is more rapid and the time to reach equilibrium value is shorter as the mobility of the photoelectron is increased. The final current is the result of a delicate balance between the voltage drops in the neutral region II and the bleached region I.

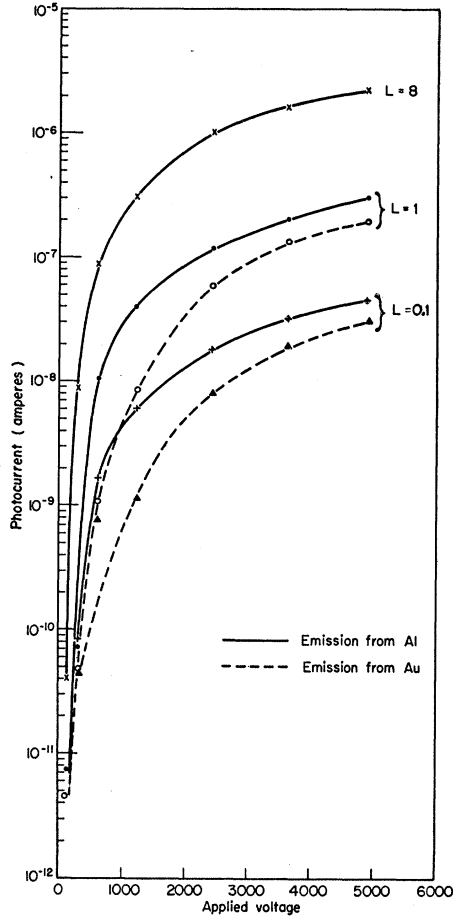


FIG. 7. Final photocurrents as a function of voltage at different light intensities.

Increase of the light intensity raises the conductivity of the crystal by increasing the electron mobility,³ and readjusts the potential gradients for a higher current level.

4. Electron Emission as a Function of Temperature

The emission from a silver electrode at room temperature and at -130°C is shown in Fig. 9. The difference between the two curves amounts to a factor of only about two. Thus, as expected, the photocurrents are dominated by high field emission, and thermionic

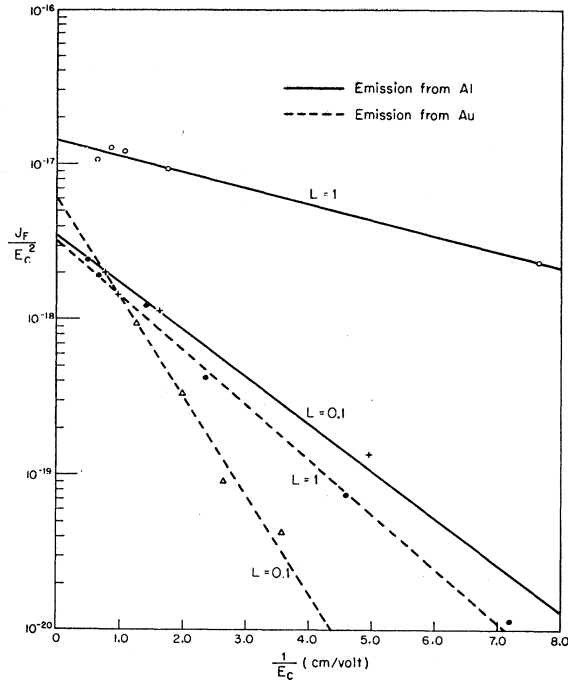


FIG. 8. Fowler-Nordheim plot for final photocurrents.

emission into the crystal plays no role. The increase of current at the higher temperature can be ascribed to an increase of electronic mobility.

Hereafter, the crystal temperature was kept at -130°C in order to suppress secondary effects, such as ionic conduction and the thermal ionization of F-centers.

5. Final Photocurrents in a Fowler-Nordheim Plot

In the usual field emission experiments from metals into vacuum, the currents are measured as a function of the field at the cathode and a Fowler-Nordheim plot yields a value for the work function. Figure 7 shows the final photocurrents as a function of applied voltage for three different light intensities and for gold and aluminum electrodes. When the cathode field, E_c , is calculated according to Eq. (16), a series of straight lines is obtained (Fig. 8). The constants a and b of the Fowler-Nordheim equation,

$$J_F = aE_c^2 e^{-b/E_c} \tag{18}$$

are given in Table III.

TABLE II. Comparison of $I(0)_{\text{charging}} - I_F$ with $I(0)_{\text{discharging}}$.

Voltage	I_F amp	$I(0)_{\text{charging}}$ amp	$I(0) - I_F$ charging amp	$I(0)_{\text{discharging}}$ amp (measured)
4900	3.5×10^{-7}	5.6×10^{-7}	2.1×10^{-7}	1.7×10^{-7}
2450	1.4×10^{-7}	2.7×10^{-7}	1.3×10^{-7}	1.0×10^{-7}
610	0.93×10^{-8}	4.1×10^{-8}	3.2×10^{-8}	3.3×10^{-8}
300	0.05×10^{-8}	1.8×10^{-8}	1.75×10^{-8}	1.7×10^{-8}
113	7.6×10^{-12}	6.6×10^{-9}	6.6×10^{-9}	6.7×10^{-9}

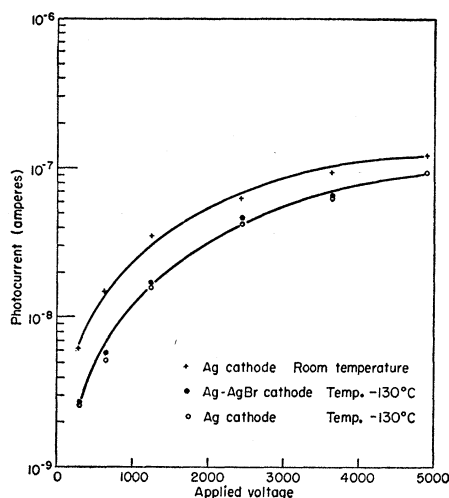


FIG. 9. Final photocurrents at a constant light intensity.

Several interesting observations can be made. The derived cathode fields are of the order 10^4 to 3×10^5 v cm^{-1} . At the higher values, close to the breakdown strength of the crystal, some of the instabilities, as observed by von Hippel¹ in his prebreakdown current measurements, were noted. This gives us some confidence in the accuracy of the calculation.

The experimental value of a yields an effective emitting area of 10^{-11} cm^2 . The numerical value of b represents an "apparent work function" for the metal-insulator contact of the order of 0.01 ev. Even though the Fowler-Nordheim equation is valid only for emission into vacuum it is difficult to see how the insulator could change a work function of about 4 ev to such a low value.

Qualitatively, the results are as follows:

(1) The final photocurrents are field emission currents.

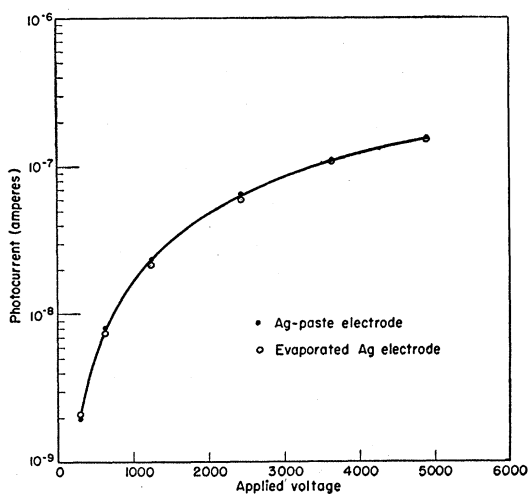


FIG. 10. Final photocurrents at a constant light intensity.

(2) The apparent work function of the metal insulator, contained in the constant b , is a function of the light intensity.

(3) The observed work functions, cathode fields and effective emitting areas are much too small from the standpoint of a standard field-emission theory.

6. Effect of the Work Function of the Metal on Emission

At this point, it was suspected that the work function of the metal exerts a very minor influence on the emission characteristics. The final photocurrents at constant light intensity were therefore measured for crystals with different metal electrodes. Silver served as the reference electrode, calcium, magnesium, and copper as counterelectrodes. The maximum asymmetry in forward and reverse current for these electrode systems proved smaller than that of Fig. 7 for gold and aluminum electrodes.

7. Field Emission from Composite Films

A series of experiments were made with silver electrodes by varying the nature and composition of their contact with the crystal. Emission from these surfaces was compared with that from a normal, vacuum-deposited silver electrode. Figure 9 compares the current-voltage characteristics for an Ag-AgBr film and an Ag film. The Ag-AgBr layer was produced by evaporating a thin layer (*ca* 100 Å) of Ag on the crystal, exposing it to bromine vapor at room temperature for one hour, and then covering it with another thin layer of Ag by evaporation. The two emission curves coincide.

Identical results were obtained in the comparison of evaporated Ag *vs* Ag paste (backed with evaporated Ag) (Fig. 10); Ag on a freshly cleaved surface *vs* Ag on a water-polished surface produced a somewhat higher emission (Fig. 11). An Ag_2O electrode, formed by subjecting a thin layer of evaporated silver to a glow discharge in oxygen and then topping it with a second silver layer, again gave no difference.

8. Effect of Hydrogen Treatment on Emission

Curve I(a) of Fig. 12 represents a typical current-voltage curve of the type discussed thus far. Heating

TABLE III. Experimental values of the Fowler-Nordheim coefficients [Eq. (18)].

Al cathode	a (ohm-volt) ⁻¹	b volt cm^{-1}
$L=1$	1.4×10^{-17}	1.0×10^4
$L=0.1$	3.5×10^{-18}	3.0×10^4
Au cathode I		
$L=1$	3.2×10^{-18}	3.5×10^4
$L=0.1$	6.1×10^{-18}	6.3×10^4
Au cathode II		
$L=1$	2.3×10^{-20}	3.6×10^4
$L=0.1$	8.6×10^{-20}	6.7×10^4

this crystal, with its electrodes in place, in an atmosphere of hydrogen for 2 hr at 200°C drastically reduces the emission from both electrodes [curve I(b)]. Evaporating only one electrode, heat-treating the crystal in hydrogen as before, and then evaporating the other electrode still reduces the emission from both electrodes (curve II). To produce an asymmetry in emission, i.e., a rectifier operating with photoconductive field emission, it was necessary to split the crystal after treatment. In this case, a nontreated surface [curve III(a)] opposed a hydrogen-treated surface [curve III(b)]. It made no difference whether the silver was evaporated on the crystal before or after hydrogen treatment.

These experiments demonstrate that the reduction of current by hydrogen treatment is caused by a change in the properties of the crystal surface layer; the bulk properties of the crystal, the F -center concentration, as measured optically by a recording spectrophotometer or photoelectrically by the initial currents $I(0)$, remained unaltered. Undoubtedly, the U -center concentration increased sharply in the surface layer, as hydrogen diffused into the crystal.⁹

9. Measurements on a Noncolored Crystal

Room-temperature measurements were made with a clear KBr crystal (length=0.1 mm). The maximum voltage available (5000 v) produced, with illumination, currents of the order of 10^{-10} amp which were very erratic. This illustrates the power of the method of utilizing space charge to increase the cathode field to field emission. With a colored crystal, currents as high as 10^{-6} amp could be drawn with much less noise.

At 300 v, the clear crystal showed a photoresponse of ca 5×10^{-12} amp. This sensitivity was traced to a residual F -band absorption. No evidence of external photoeffect from the metal cathode was obtained. This

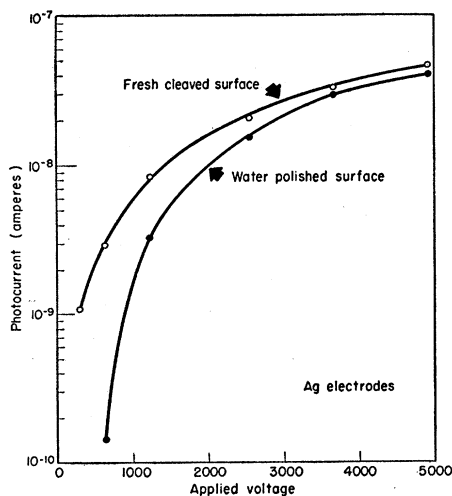


FIG. 11. Final photocurrents at a constant light intensity.

⁹ R. Hilsch and R. W. Pohl, *Trans. Faraday Soc.* **34**, 883 (1938).

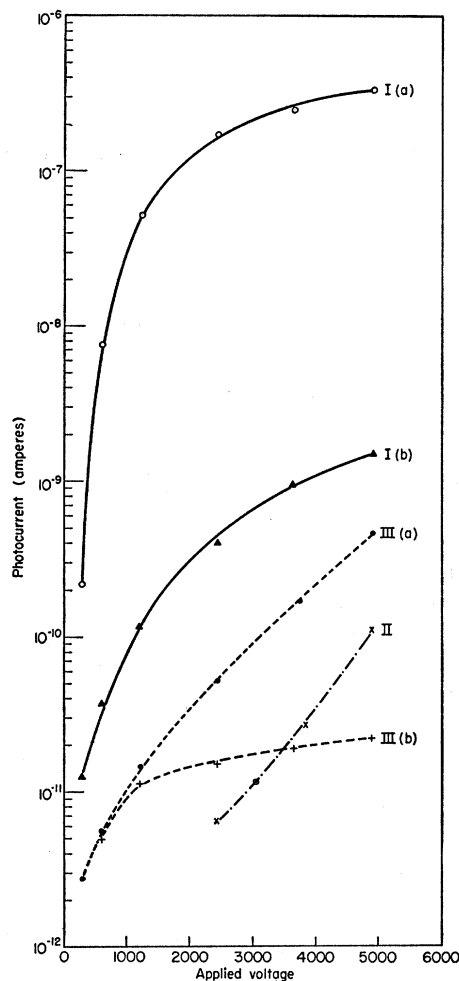


FIG. 12. Effect of hydrogen treatment on emission characteristics.

is consistent with Gilleo's results,¹⁰ that the photoemission from Ag into KBr requires 4.3 ev.¹⁰ Our light source did not extend to this energy range.

DISCUSSION

The salient experimental facts are as follows:

- (1) The magnitude of the apparent work function decreases with increasing light intensity.
- (2) The work function of the metal does not influence the current emission.
- (3) Hydrogen treatment affects the surface of the crystal and decreases the emission.
- (4) The calculated values of the cathode field, the apparent work function and the emitting area are too small.

We have dealt with the positive space charge as a continuous layer producing a uniform field at the metal surface. This macroscopic theory fails when the distance

¹⁰ M. A. Gilleo, *Phys. Rev.* **91**, 534 (1953).

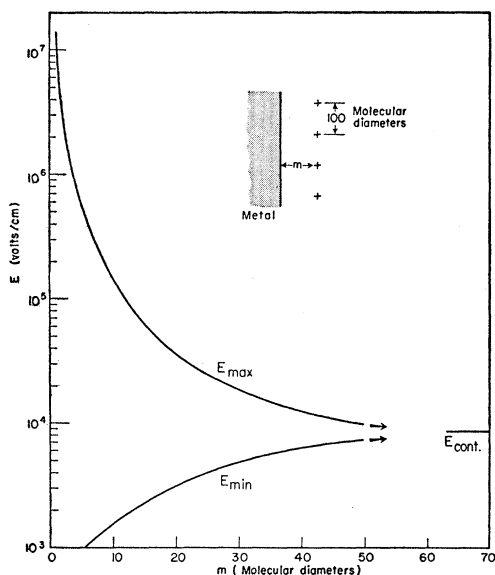


FIG. 13. The maximum and minimum fields at a metal from a grid network of positive points.

between neighboring charges is large in comparison with their distance to the cathode. In this case the field at the metal is nonuniform, and may be larger than that indicated by the macroscopic theory.

For the concentration of F -centers used (10^{16} cm^{-3}), the average distance between neighboring centers is of the order of 100 molecular diameters. The electric fields at a metal surface produced by a two-dimensional grid network of positive points, with this order of spacing, is shown in Fig. 13. E_{max} and E_{min} are the maximum and minimum fields at the metal: the points of projection of a positive charge and the center of the square of four positive charges. As the distance of the grid to the metal increases, E_{min} approaches E_{max} , and both fields approach the value of the field from a continuous charge sheet, E_{cont} . E_{max} was calculated by summing the contributions from 25 neighboring charges and their images. Thirty-six charges, with their images were used to calculate E_{min} .

For $m \leq 10$ molecular diameters, the maximum field at the metal is approximately that of a point charge and its image:

$$E_{\text{max}} \simeq (1/4\pi\epsilon') (2e/m^2). \quad (19)$$

For an ionized F -center within 1 molecular diameter from the metal, this field is about 10^7 v cm^{-1} . Here, obviously, is the source of the high electric field strength necessary for cold emission. Beyond 10 molecular diameters ($\sim 10^{-7} \text{ cm}$), the image forces are reduced to less than 10^5 v cm^{-1} , and the macroscopic theory becomes valid.

Region I, the bleached section of the crystal, therefore has to be divided into two sections (Fig. 14):

- (1) Region I_a , a thin layer adjacent to the metal, of

width about 10^{-7} cm , containing the first layer of positive charge.

- (2) Region I_b , of width about 10^{-3} cm , with the remainder of the positive charge.

A simple phenomenological analysis will illustrate the important features of electron trapping and release in region I_a . In the Fowler-Nordheim derivation of cold emission from metals into vacuum, the current density is given by:

$$J = \int_0^{\infty} \alpha(E)n(E)dE, \quad (20)$$

where $n(E)$ is the number of electrons per cm^2 per sec arriving at the metal surface with energies between E and $E+dE$, and $\alpha(E)$ is the probability of escape of an electron through the surface barrier; α is an explicit function of the metal work function ϕ .

When an insulator is adjacent to the metal, Gilleo,¹⁰ in his experiments on the determination of the photoelectric work function of Ag on KBr, showed that the electrons ejected from the metal are trapped near the cathode at anion vacancies and are released further into the crystal by F -band illumination. In our case, preferred trapping sites are the points of positive space charge, the ionized F -centers in region I_a . The greater their density, the greater is the emission current from the metal:

$$J_1 = \beta n N_e, \quad (21)$$

where J_1 is the current density from metal into region I_a , N_e is the time average of the number of ionized F -centers, and β is the transmission coefficient per ionized F center for an electron striking the metal-insulator interface. Thus

$$\begin{aligned} J_1 &= \alpha n, \\ \alpha &= \beta N_e, \end{aligned} \quad (22)$$

where α , as defined above, is the probability of escape of an electron from the metal.

Release of electrons from region I_a into the bulk of the crystal is accomplished only photoelectrically. The current is proportional to the number of occupied centers in region I_a and the light intensity; therefore

$$J_2 = L\gamma(N - N_e), \quad (23)$$

where L is the number of photons absorbed per cm^2 per sec in region I_a , N is the total number of F centers in region I_a , $N - N_e$ is the time average of the number of occupied F centers in region I_a , and γ is the probability of escape into region I_b per photon per occupied F center. γ will increase as the macroscopic field in region I_b increases. For equilibrium,

$$\begin{aligned} J_1 &= J_2, \\ \beta n N_e &= \gamma L(N - N_e), \end{aligned} \quad (24)$$

$$N_e = \frac{N}{1 + (\beta n / \gamma L)}$$

hence

$$\alpha = \frac{N}{(1/\beta) + (n/\gamma L)}. \quad (25)$$

The transmission coefficient α is now an explicit function of the light intensity. As the light intensity L increases, α increases, and the apparent work function decreases. A greater number of F -centers are ionized per second in region I_a , and subsequently more escape into region I_b . This larger current can be transferred through the bulk of the crystal by the increase of the mobility of the electrons, which is defined, according to von Hippel,¹ as the average drift distance in the field direction w , divided by the time t_f the electron moves free plus the time t_b the electron stays bound in its trap

$$b = w / (t_f + t_b). \quad (26)$$

It is the time t_b which is shortened by increase of the light intensity.

At any particular light intensity there is a balance between the neutralization of the positive charge N_e in region I_a by electrons from the cathode, and the replenishment of this charge by photonrelease of electrons into region I_b . When the applied voltage is raised, the width of the space-charge layer in region I_b , and the electric field associated with it increase. The probability of escape of electrons from region I_a , γ , is enhanced by this larger driving field and the current level increases.

Electrons released by photons in region I_a are under the influence, not only of the space-charge fields of region I_b , but also of their image fields which tend to pull them back into the metal. If most of the photoelectrons return to the metal or are retrapped at other sites in the layer I_a and only a small fraction escapes into region I_b ,

$$\beta n \gg L\gamma; \quad (27)$$

hence

$$\alpha \approx N\gamma L/n. \quad (28)$$

The transmission probability α , is then independent of the term β , which contains the work function of the metal.

The diffusion of hydrogen into the surface transforms the F -centers into U -centers. The latter, absorbing in the far ultraviolet, do not release photoelectrons, and

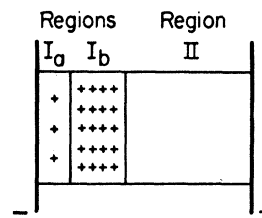


Fig. 14. Space-charge distribution with field emission.

consequently the current decreases with hydrogen treatment.

Another point of view, consistent with the macroscopic field calculation, is to consider the metal-insulator boundary as the interface between regions I_a and I_b . The surface of the metal is contaminated with a thin dielectric layer (region I_a) with an enclosed positive charge. A small voltage drop and a high field strength appear across this insulating layer. The calculated work function and cathode fields have to be modified for this redefined metal-insulator contact. An increase of light intensity increases the positive space charge and the potential drop in the dielectric film; the apparent work function decreases.

The results are in good agreement with the experiments of field emission from metals into gases,¹¹ and into liquids.¹² Here again the macroscopic values of electric field, the emitting areas, and the calculated "apparent work function" of the metal surface were reported as too small to be reasonable. The mechanism responsible for emission is assumed to reside in a positive-ion space charge adjacent to a thin film on the metal.

ACKNOWLEDGMENTS

The author wishes to express his indebtedness to Professor A. R. von Hippel for his guidance and illuminating suggestions, which provided the solution to several aspects of this problem; to D. A. Powers, group leader of the High-Voltage Section, for invaluable assistance in the experimental phases of this project; to J. Kalnajs for his help in problems of a chemical nature; and to V. Sils for aid in the preparation of the colored crystals.

¹¹ F. Llewellyn-Jones and E. T. de la Perrelle, Proc. Roy. Soc. (London) **A216**, 267 (1953); F. Llewellyn-Jones and C. G. Morgan, Proc. Roy. Soc. (London) **A218**, 83 (1953).

¹² W. B. Green, Technical Report 93, Laboratory for Insulation Research, Massachusetts Institute of Technology, March, 1955 (unpublished).